

IDENTIFYING AND MAPPING SYSTEMATIC ERRORS IN PASSIVE MICROWAVE SNOW WATER EQUIVALENT OBSERVATIONS

¹James Foster, ^{2,3}Chaojiao Sun, ⁴Jeffrey P Walker, ^{1,3}Richard Kelly, ^{1,3}Jairui Dong, and ¹Alfred Chang

¹*Hydrological Sciences Branch, Laboratory for Hydrospheric Processes
NASA Goddard Space Flight Center, Greenbelt, Maryland, 20771 USA*

²*Global Modeling and Assimilation Office
NASA Goddard Space Flight Center, Greenbelt, Maryland, 20771 USA*

³*Goddard Earth Sciences and Technology Center
University of Maryland Baltimore County, Baltimore, Maryland 21250, USA*

⁴*Department of Civil and Environmental Engineering
University of Melbourne, Parkville, Victoria, 3010 Australia*

KEYWORDS: passive microwave, snowpack, snow crystals, systematic errors, snow water equivalent

ABSTRACT:

Understanding remote sensing retrieval errors is important for correct interpretation of observations, and successful assimilation of observations into numerical models. Passive microwave sensors onboard satellites can provide global snow water equivalent (SWE) observations day or night and under cloudy conditions. However, there are errors associated with the passive microwave measurements, which are well known but have not been adequately quantified so far. This study proposes a new algorithm for passive microwave SWE retrievals that removes known systematic errors. Specifically, we consider the impact of vegetation cover and snow crystal growth on passive microwave responses. As a case study, systematic errors (difference between the old and new algorithms) are presented for the snow season 1990-91. Standard error propagation theory is used to estimate the uncertainty in the new retrieval algorithm (not shown here). An unbiased SWE dataset is produced and monthly SWE error maps (October-May) are derived for the Northern Hemisphere. The next step is to fine tune and test the bias-free algorithm, which will be applied to the combined passive microwave dataset from SMMR and SSM/I over 20 years.

I. INTRODUCTION

Snow plays an important role in the global energy and water budgets, as a result of its high albedo and thermal and water storage properties. Snow is also the largest varying landscape feature of the Earth's surface. Thus, knowledge of snow extent and SWE are important for climate change studies and applications such as flood forecasting. Furthermore, snow depth and SWE, as well as snow cover extent, are important contributors to both local and remote climate systems.

Despite its importance, the successful forecasting of snowmelt using atmospheric and hydrologic models is challenging. This is due to imperfect knowledge of snow physics and simplifications used in the model, as well as errors in the model forcing data. Furthermore, the natural spatial and temporal variability of snow cover is characterized at space and time scales below those typically represented by models. Snow model initialization based on model spin-up will be affected by these errors. By assimilating snow observation products into Land Surface Models (LSMs), the effects of model initialization error may be reduced (Sun et al., 2003).

Passive microwave remote sensors onboard satellites provide an all-weather global SWE observation capability day or night. Brightness temperatures from different channels of satellite passive microwave

sensors (hereafter referred to as PM) can be used to estimate the snow water equivalent (or snow depth with knowledge of the snow density), and hence snow cover extent. However, there are both systematic (bias) and random errors associated with the passive microwave measurements. In order for the remotely sensed SWE observations to be useful for climate modelers, water resource managers and flood forecasters, it is necessary to have both an unbiased SWE estimate and a quantitative, rather than qualitative, estimate of the uncertainty. This is a critical requirement for successful assimilation of snow observations into LSMs.

For most PM algorithms, the effects of vegetation cover and snow grain size variability are the main source of error in estimating SWE. Of lesser concern are the effects of topography and atmospheric conditions. A major assumption made in a number of PM algorithms is that vegetation cover does not affect the SWE estimates. In fact, it can have a significant impact on the accuracy of SWE estimates. In densely forested areas, such as the boreal forest of Canada, the underestimation of SWE from retrieval algorithms can be as high as 50% (Chang et al., 1996). Another major assumption is that snow density and snow crystal size remain constant throughout the snow season everywhere on the globe; in reality, they vary considerably over time and space. The PM algorithms

are found to be very sensitive to snow crystal size (Foster et al., 1999).

$$SWE = c (T_{19} - T_{37}) \quad [mm] \quad (1)$$

The purpose of this paper is to present a methodology for deriving unbiased SWE estimates from PM observations. Systematic errors due to simplifying assumptions of the retrieval algorithm and effects of vegetation cover and crystal size are quantified. This paper presents results for the snow season 1990-91 as an example, using Special Sensor Microwave/Imager (SSM/I) data.

2. PASSIVE MICROWAVE RADIOMETRY

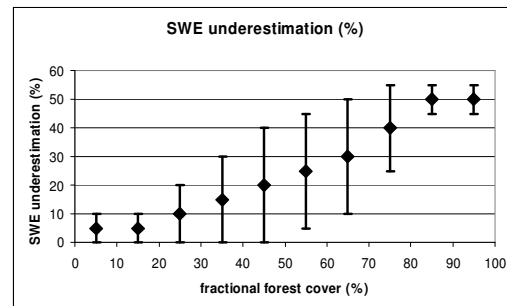
If a snowpack is not too shallow (> 5 cm or contains more than about 10 mm SWE), scattering of naturally emitted microwave radiation by snow crystals occurs and can be detected at frequencies greater than about 25 GHz. Otherwise, the snow will be virtually transparent. By comparing brightness temperatures detected at an antenna at frequencies greater than 25 GHz (typically scattering dominated) with those brightness temperatures detected at frequencies less than 25 GHz (typically emission dominated), it is possible to identify scattering surfaces. Generally, the strength of scattering signal is proportional to the SWE, and it is this relationship that forms the basis for estimating the water equivalent (or thickness) of a snow pack (Chang et al., 1976; Pulliainen and Hallikainen, 1999; Tsang et al., 2000; Kelly et al., 2003).

From November 1978 to the present, the SMMR instrument on the Nimbus-7 satellite, and the SSM/I on the Defense Meteorological Satellite Program (DMSP) series of satellites have acquired PM data that can be used to estimate SWE. The SMMR instrument failed in 1987, the year the first SSM/I sensor was placed in orbit. On SMMR, the channels most useful for snow observations are the 18 and 37 GHz channels. For the SSM/I, the frequencies are slightly different (19.35 and 37.0 GHz). The data are projected into ½ degree latitude by ½ degree longitude grid cells, uniformly subdividing a polar stereographic map according to the geographic coordinates of the center of the field of view of the radiometers. Overlapping data in cells from separate orbits are averaged to give a single brightness temperature, assumed to be located at the center of the cell (Armstrong and Brodzik, 1995, Chang and Rango, 2000).

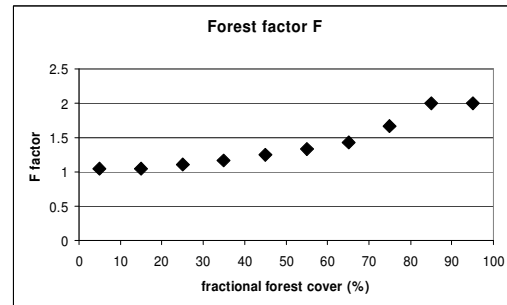
We propose a modified SWE algorithm based on the original algorithm by Chang et al. (1987), where brightness temperature differences between the 19 GHz (or 18 GHz for SMMR) and 37 GHz channels are multiplied by a constant related to the average grain size to derive the water equivalent of the snowpack. The simple algorithm is

where SWE is snow water equivalent in mm, c is 4.8 mm K⁻¹, and T_{19} and T_{37} are the horizontally polarized brightness temperatures at 19 GHz (or 18 GHz for SMMR) and 37 GHz, respectively. The performance of this algorithm is similar when either vertical or horizontal polarizations are utilized – horizontal polarization was used in this study (Rango et al., 1979). If the brightness temperature from the 19 GHz channel is less than that from the 37 GHz channel, then the snow depth and SWE are zero.

To derive snow depth, SWE is simply divided by the snow density. It has been determined that in general, a snow density value of 300 kg/m³ is representative of mature mid winter snow packs in North America (Foster et al., 1996). The effect of this is to modify the coefficient in (1) such that c is 1.60 cm K⁻¹ (1.59 cm K⁻¹ for SMMR).



(a)



(b)

Figure 1. (a) Underestimation of SWE due to forest cover. The error bars denote uncertainty of the underestimation. (b) The forest factor F as a function of fractional forest cover.

3. A NEW RETRIEVAL ALGORITHM

There are typically two kinds of errors associated with a given observation, systematic error (bias) and random error. In this study, the emphasis is to evaluate the bias in the original algorithm (1) by comparing with a new algorithm (2). We use the term “bias” as if the new algorithm gives the “true” values of SWE.

3.1 Error due to forest cover

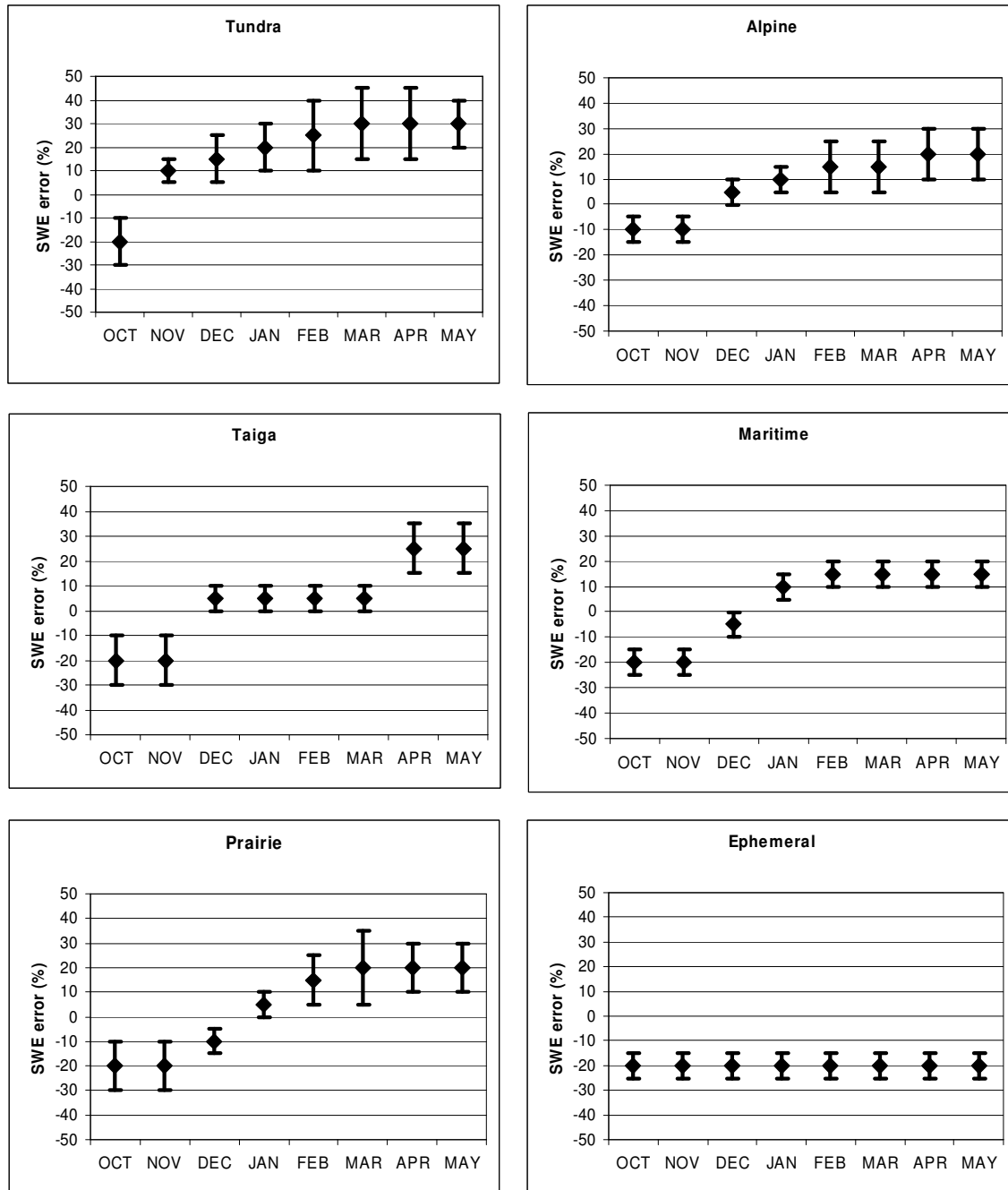


Figure 2. SWE overestimation or underestimation for the six Strum classes due to the assumption of constant grain size.

The primary source of systematic error in SWE is the masking effect of vegetation, which reduces the brightness temperature difference term in (1). In the PM portion of the electromagnetic spectrum, the error due to forest cover is expected to be very high, upwards of 50%, since the emissivity of the overlying forest canopy can overwhelm the scattering signal from the snowpack (Chang et al., 1996; Brown et al., 2003). Where forests are scant or absent PM estimates of SWE are more accurate.

For each forested pixel, a *fractional forest cover* fr is calculated using the International Geosphere-Biosphere Program (IGBP) Land Cover Data Set described by Loveland et al. (2000). These data, at 1 km x 1 km, are averaged to the 1° x 1° latitude/longitude grid used in this study. The percentage of forest cover in a PM pixel was calculated from the total number of forest classification pixels at 1 km divided by the total number of pixels. Based on this fractional forest cover, the systematic error in the SWE value obtained from

(1) can be estimated. A multiplicative “forest factor” F is introduced to remove the bias due to forest cover from (1)

$$SWE = F c (T_{19} - T_{37}) \quad [mm]. \quad (2)$$

We derived the values of forest factor F by assigning underestimation errors for algorithm (1). In Figure 1a, the diamonds denote the underestimation error in (1) due to forest cover. For example, if the fractional forest cover at a given pixel is 65%, we assume (1) underestimates SWE by 30%. These nonlinear values are inexact, but are our best approximations at this time. The error bars are our estimates of uncertainty associated with the underestimation estimate of a particular forest cover fraction. The more mixed the pixel, the more uncertainty there is on the forest influence of the PM signal. In other words, untangling the contribution of the signal due to scattering from the underlying snow and emission from trees is harder to assess when the mixture is more even.

Figure 1b shows the forest factor F as a function of fractional forest cover f_r in North America (maximum of 2.0). Note that the F factor increases (nonlinearly) with forest cover. This is to correct for more severe underestimation of SWE due to dense forest cover. The values for F are based on the underestimation of SWE at different values of f_r .

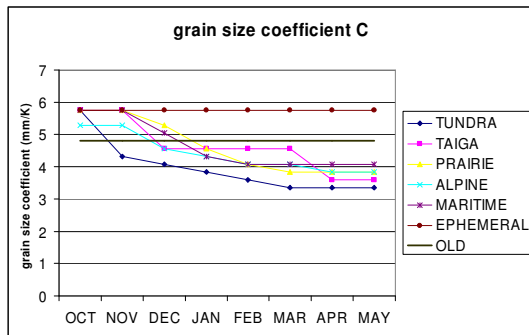


Figure 3. Monthly grain size coefficient c for six Sturm classes. The constant value 4.8 (mm/K) used in the original algorithm is also plotted and labeled as “OLD”.

3. 2 Error due to grain size variability

The secondary source of SWE error results from the retrieval algorithm assumption that snow crystal size and shape is spatially uniform and remains constant throughout the snow season. This assumption is reflected in the original SWE retrieval algorithm (1) where c is a constant. The constant coefficient c (4.8 mm K⁻¹) is associated with an average crystal size of 0.3 mm (radius). In fact, snow crystals vary with location and evolve with time. Since microwave scattering increases as the crystals grow in size as the snow season progresses, the algorithm (1) typically overestimates SWE, except when the snowpack is thin.

Sturm et al. (1995) have characterized the seasonal snowpack into six classes (excluding continental ice caps and ocean/water bodies), based on vegetation and meteorological conditions: tundra, taiga, alpine, prairie, maritime and ephemeral. In this investigation, we use these classes to address the issue of spatial inhomogeneity of snowpacks. In addition, we consider the evolution of snow crystal size of these different snow classes. As a result, the c value used in (2) now varies with location and time.

In this study, it is assumed that crystals grow throughout the snow season – an exception to this is the “ephemeral” snow class. Where temperature and vapor gradients are greater (northern interior climates – taiga, tundra, and prairie snow classes), the rate of growth and the associated crystal size errors are typically larger.

Figure 2 shows the systematic errors for six different “Sturm” snow classes due to grain size variability. For each Sturm snow class calendar month, a percentage error in SWE due to differences in snow crystal size over time is prescribed. They are assigned based on various field campaign results with snow crystal samples collected and analyzed, as well as subjective analysis (based on previous work and personal field experience). Negative values denote underestimation of SWE, while positive values denote overestimation. The greatest systematic error occurs in the tundra snow and the least in maritime or ephemeral snow. The largest uncertainty in c random errors occur in the tundra and prairie during the late winter and early spring period, whereas the smallest uncertainty is for the maritime and ephemeral snow classes.

Note that for November, (1) underestimates SWE for each snow class. That is because when the snow cover is shallow (< 5 cm), as it generally is at the beginning of the snow season, microwave radiation at all observed frequencies passes through the snowpack virtually unimpeded.

Figure 3 shows the different values of c for each of the six Sturm snow classes for each month of the snow season from October to May for North America. These values are derived from estimates of snow crystal size-related errors (Fig. 2). When the average crystal size is smaller than 0.3 mm, c becomes larger than 4.8; when the crystal size is larger, c becomes smaller.

In summary, to compute unbiased SWE value for each pixel using (2), the forest factor F is first determined based on the forest cover fraction of this pixel, and then the c value is assigned based on its snow class category and time of the year. The introduction of forest factor F and time- and space-varying c in (2) is to correct the systematic errors in (1) so that only random errors remain.

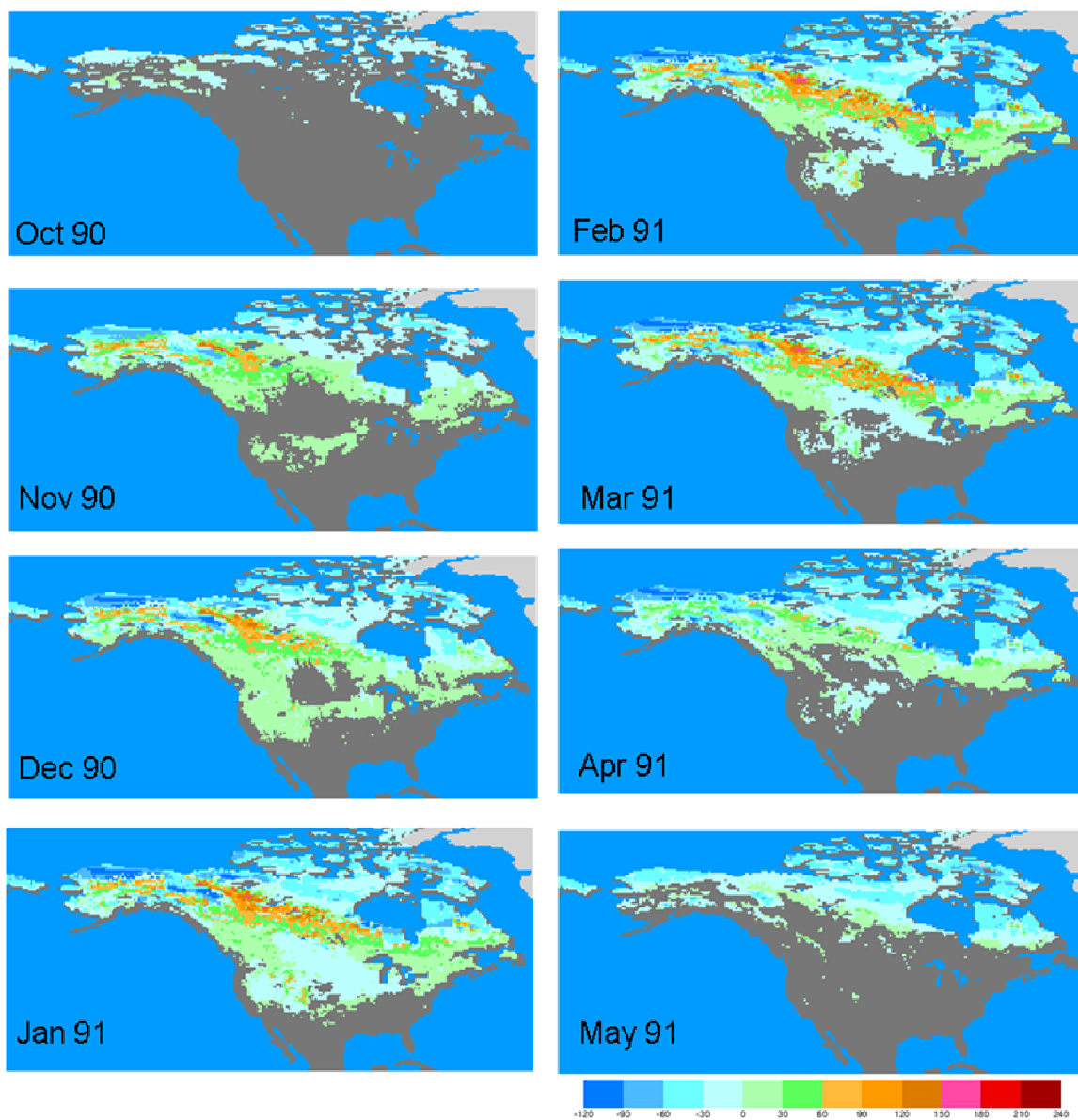


Figure 4: Difference maps between the new and old SSM/I SWE algorithms for October 1990 through May 1991.

3.3 Comparisons between the new and old algorithm for SWE retrieval

Figure 4 shows maps of monthly biases, i.e., difference between SWE estimate from the new (2) and old algorithm (1). Shades of blue indicate that the new algorithm is estimating less snow than the original global snow algorithm, while shades of red indicate that the new algorithm is estimating more. The pale blue and sage colors in Figure 6 indicate areas where there is little difference in SWE estimates by the two algorithms. Because snow crystals are typically larger in tundra regions than in forested regions, snow thickness and SWE were overestimated

using the original algorithm. Snow was underestimated using (1) in forested areas because the microwave emission from the trees was overwhelming scattering from the underlying snowpack. The most noticeable negative values are found in the northern portion of the Mackenzie River basin and on the north slope of Alaska. With the inclusion of a forest factor in the new algorithm, considerably more SWE is estimated in the taiga or boreal forest region.

4. CONCLUSIONS

This study corrects an existing SWE model for known systematic errors. Dense vegetation was shown to be the major source of systematic error, while assumptions about snow crystal size and how crystals evolve with the progression of the season also contribute significant biases. The proposed unbiased algorithm is applied to SSM/I data in a case study for snow season 1990-91, with an associated uncertainty estimate (not shown here). These results have been evaluated in taiga, prairie and maritime regions of Canada using snow data from the Meteorological Service of Canada. In the most densely forested areas of the taiga and maritime classes of eastern Canada, SWE may still be underestimated using the new algorithm. As more complete data on forest density becomes available, separate forest factors could be prescribed for taiga and maritime sub-classes to better account for SWE in densely forested areas.

Acknowledgements

This work was performed under the auspices of NASA Grant NASA NRA 99-OES-04.

References

- Armstrong, R. L. and M. J. Brodzik, 1995: An earth-gridded SSM/I data set for cryospheric studies and global change monitoring, Advances in Space Research Vol. 10, 155-163.
- Brown, R., B. Brasnett and D. Robinson, Gridded North American monthly snow depth and snow water equivalent for GCM evaluation, Atmos.-Ocean, Vol. 41, 1-14, 2003.
- Chang, A. T. C., P. Gloersen, T. Schmugge, T. Wilhelm, and J. Zwally, 1976: Microwave emission from snow and glacier ice, Journal of Glaciology, Vol. 16, 23-39.
- Chang, A.T.C., J.L. Foster and D.K. Hall, 1987: Nimbus-7 derived global snow cover parameters, Annals of Glaciology, Vol. 9: 39-44.
- Chang, A.T.C., J.L. Foster and D.K. Hall, 1996: Effects of forest on the snow parameters derived from microwave measurements during the BOREAS winter field experiment, Hydrological Processes, Vol.10: 1565-1574.
- Chang, A.T.C. and Rango, A., 2000: Algorithm Theoretical Basis Document (ATBD) for the AMSR-E Snow Water Equivalent Algorithm, NASA/GSFC, Nov. 2000.
- Foster, J. L., D. K. Hall, A. T. C. Chang, A. Rango, W. Wergin, and E. Erbe, 1999: Effects of snow crystal shape on the scattering of passive microwave radiation, IEEE Transactions on Remote Sensing, Vol.37 (2), 1165-1168.
- Kelly, R., and A. Chang, L. Tsang, and J. Foster, 2003: A prototype AMSR-E global snow area and snow depth algorithm, IEEE Transactions on Geoscience and Remote Sensing, Vol. 41 (2), 230-242.
- Loveland, T. R., B. C. Reed, J. F. Brown, D. O. Ohler, J. Zhu, L. Yang, and J. W. Merchant (2000): Development of a global land cover characteristics dataset, International Journal of Remote Sensing, Vol. 21 (6/7), 1303-1330..
- Pulliainen, J. and M. Hallikainen, 2001: Retrieval of regional snow water equivalent from space-borne passive microwave observations, Remote Sensing of Environment, Vol. 75: 76-85.
- Rango, A., A. Chang, J. Foster, 1979: The utilization of space-borne radiometers for monitoring snowpack properties, Nordic Hydrology, Vol. 10, 25-40.
- Sturm, M., J. Holmgren and G. E. Liston, 1995: A seasonal snow cover classification system for local to regional applications, Journal of Climate, Vol. 8, 1261-1283.
- Sun, C., J. Walker and P. Houser, 2003: A methodology for initializing snow in a global climate model: Assimilation of snow water equivalent observations. J. Geophys. Res. (In press).
- Tsang, L., C. Chen, A.T.C. Chang, J. Guo and K. Ding, 2000: Dense media radiative transfer theory based on quasicrystalline approximation with applications to passive microwave remote sensing of snow, Radio Science, Vol. 35: 731-749.